High Resolution Cross-Well Imaging of a West Texas Carbonate Reservoir: Part 3. Wavefield Separation

BG1.4

J. W. Rector III, Univ. of California, Berkeley (formerly Stanford Univ.); S. K. Lazaratos, J. M. Harris, and M. Van Schaack, Stanford Univ.*

SUMMARY

A well to well seismic survey was acquired in a West Texas oil field in 1991. This crosswell field experiment was acquired in a manner that permitted P-P and S-S reflection arrivals to be extracted from the complex total wavefield. In this paper and the following one, we discuss the extraction and the imaging of the reflection arrivals for the crosswell seismic data. This paper focuses on the wavefield separation and deconvolution of the data. Although reflections are barely distinguishable in the raw data, through adaptive multichannel filters applied in the domains of common source, receiver and vertical offset, we are able to produce reflection wavefields that are highly continuous, with a minimum amount of Rieber mixing. The techniques used in this work require data volumes and associated data filtering operations that are several orders of magnitude larger than those encountered in conventional VSP data analysis. In many respects, this aspect makes data manipulations more similar to conventional surface seismic processing than to VSP processing.. The high quality of the S-S reflections imaged from single component borehole hydrophone data in this experiment may reduce the use of multicomponent sources and receivers for some crosswell applications.

INTRODUCTION

Several authors have recently proposed using crosswell reflection arrivals to image the subsurface between two boreholes (Lazaratos et al, 1991 and Stewart and Marchisio, 1991). Well-to-well imaging with reflections holds several advantages over more conventional transmission tomography techniques. First and foremost, reflections provide an image of horizons at and below the well bottom, where the target (i. e. the reservoir) is typically located. Transmission tomography is limited to zones above the well bottom. Figure 1 shows the zone imaged with transmission tomography compared to the zone imaged with reflections for a single common source gather assuming horizontal reflectors in a constant-velocity earth. (A reciprocal common receiver gather would yield a zone of coverage that is mirrored across a vertical line at the midpoint between the two wells.) Note that only the reflection arrivals image a significant horizontal portion of the subsurface near the bottom of the well and below.

This paper is the first of two papers that discuss the reflection image processing performed on crosswell seismic data acquired at a West Texas oil field. The extraction of P-P and S-S reflections through wavefield separation and deconvolution are summarized in this paper. Through adaptive multichannel filtering applied in common source, receiver and offset domains, reflected arrivals can be identified that correspond closely with interfaces inferred from S and P velocity logs.

FULL WAVEFIELD ANALYSIS

The data acquisition parameters for this crosswell seismic are discussed in Harris et al, 1992. In the processing and analysis presented here, we will focus on the survey conducted between wells spaced 175 ft (53m). This survey, was acquired at 2.5 ft (.76 m) source and receiver intervals, substantially finer than the 10 to 20 ft (3 to 6 m) intervals commonly used in crosswell tomography surveys. The depth sampling interval was designed to allow the data to be wavefield separated, extracting reflected arrivals though moveout-based multichannel filters. With coarser sampling intervals, the slower arrivals such as the tube wave and the shear waves are substantially aliased in the frequency range of interest (300 to 2000 Hz).

Figure 2 is a typical common receiver gather. For the data shown in Figure 2, the hydrophone was located at a depth of 1904 ft (581 m), just below the top of the reservoir, and the piezoelectric source depths ranged from 1701 ft to 2101 ft (825 to 947 m). P and S-wave sonic logs from the source well are also shown. The data in Figure 2 are displayed after normalizing each trace to its maximum amplitude. P and S direct and reflected arrivals, down and upgoing P and S reflections, and converted arrivals can all be identified based on their moveout and time delay characteristics (Rector et al, 1992).

The disappearance of the shear wave in the center of the section, at small vertical source/receiver offsets, is consistent with the radiation pattern of the piezoelectric source, which can be modeled like an airgun as a radially-directed force applied to the fluid in the source well. Lee et al (1984) showed that the radiation from this type of source produces highly focused shear wave lobes with maximum radiation at +- 45 degrees, and no shear waves radiated horizontally. The P-waves on the other hand have a more uniform radiation pattern, with the largest amplitudes directed horizontally. Shear waves can be recorded by a hydrophone receiver in a borehole because a radial stress that creates a response on the hydrophone is produced by the shear body wave for every incoming direction except the radial. For more details on the radiation pattern and theoretical seismic modeling of the synthetic response for this experiment, refer to Van Schaack et al, 1992.

Another way to view the data is in common vertical offset space (Rector et al, 1992). In common offset space, the source to receiver straight line distance is constant, and the direct arrival times emulate velocity variations with depth rather than path length variations. Figure 3 is a common offset display (the offset corresponds to a straight ray angle of 63 degrees with respect to the vertical. Note that the P and S direct arrivals have similar small moveouts in this domain. The dip in arrival times in the center of the section corresponds to an area where the direct arrival was primarily travelling in the lower velocity reservoir rocks. Also note that the reflections have roughly twice as much moveout in this domain as in common receiver space.

WAVEFIELD SEPARATION

Figure 4 is a flow chart illustrating the major steps used to extract P to P reflections form the total wavefield.. A similar sequence was used to extract the S to S reflections. In the first stage of wavefield separation the direct arrival (Either P or S) was aligned as in conventional VSP wavefield separation (Hardage, 1985). A multichannel filter (filter #1) designed to attenuate zero moveout arrivals was then applied to the data. Although any type of multichannel filter (i e median, mean, f-k, τ-p, etc) could have been applied, we used a trace mix that was then subtracted from the premixed data. The length of the mix was chosen to avoid removing any primary reflection energy in the frequency band of interest (300 to 2000 Hz).

At this point notice that the data processing sequence branches. Two copies of the original data set were made: one sorted into common receiver gathers, the other sorted into common source gathers. Filter # 2 was used to attenuate reflections coming from horizontal locations near the common variable (source or receiver) borehole. This filter was also applied as a simple trace mix and subtraction. Then filter #3 was used to enhance reflections coming from locations hear the common variable well. The multichannel filter was applied as a trace mix *without* subtraction. After applying filters #2 and #3 we have two residual data sets. The one on the left side of the flowchart contains up and downgoing reflections from the half-plane on the side of the *source* well. The one on the right contains up and downgoing reflections from the half-plane on the side of the *receiver* well. Through several tests we observed that it was preferable to adaptively guide the filter pass and reject band using the direct arrival time pick rather than applying a general 2-D pie slice filter. We believe that the adaptive tuning of the filter using the direct arrival time was more important to the process than the type of multichannel filter applied.

In the final stage of wavefield separation the up and downgoing reflections were separated using *f-k* vleocity fan filters (in filter #4). By passing positive moveout arrivals we were able to extract downgoing primary reflections and by passing negative moveout arrivals we extracted upgoing reflections. Potentially, up and downgoing wavefield separation at this stage could be further improved with a more data dependent filter like the previous multichannel filters that were applied. Using a similar processing sequence with adaptive multichannel filters based on the shear wave direct arrival we isolated the shear wave reflections.

Figure 5 is a common receiver gathers after applying the sequence outlined in Figure 4 to enhance S-S upgoing reflections from horizontal locations hear the source well. These common receiver gathers correspond to the lower half of the total wavefield data shown in Figure 2. Note the excellent coherency of the upgoing reflections. Also note the minimal Rieber mixing produced. Applying wavefield separation filters using multiple sorting domains allows us to apply much milder filters than those that would be required for up and downgoing wavefield separation of VSP data, where only one sorting domain (Common source) is available.

After extracting the up and downgoing reflection arrivals, these data subsets were deconvolved. The deconvolution was performed using an operator derived from the transmission wavefield, similar to deconvolution of VSP reflection wavefields (Hardage, 1985). We obtained an estimate of the transmission wavefield by applying filter # 1 as a pass of the direct arrival rather than a rejection. Then simple predictive deconvolution using a 1 ms gap and a 10 ms operator length was applied.

The entire pre-imaging process was performed on all common receiver gathers, common source gathers, and common offset gathers (approximately 200 of each), yielding data subsets that were then imaged (see Lazaratos et al, 1992 for a discussion of the imaging results). The wavefield separation and deconvolution processing sequence represents roughly four times the number of operations required in a typical VSP processing sequence. However, in VSP we a generally dealing with only one common source gather and only one upgoing P reflection wavefield. To process all gathers and extract all reflection wavefields required about 7,500 times the amount of processing required for a single offset VSP. We performed this processing in 3 days using the ProMAX surface seismic processing system mounted on a standard UNIX workstation. Contractor processing quotes for a VSP data set of this magnitude were several hundred thousand dollars.

CONCLUSIONS

Through appropriate acquisition techniques and through the use of adaptive multichannel filtering techniques, P-P and S-S crosswell reflections were extracted from the complex total wavefield of arrivals recorded at a West Texas well-to-well field experiment. The total wavefield displays were dominated by P to S transmission and converted arrivals and exhibited relatively weak reflection signals. The data processing consisted of wavefield separation and deconvolution applied in a variety of sorting domains. The volume of data processed and the number of operations performed were between two and four orders of magnitude greater than a typical VSP, making the analysis more akin to multifold common depth point surface seismic processing than to VSP processing.

ACKNOWLEDGEMENTS

This work was supported by the sponsors of the Stanford Tomography Project, the Gas Research Institute and the David and Lucille Packard Foundation. The authors would also like to thank Chevron Oil Field Research Corporation for providing the field site and co-sponsoring the work.

REFERENCES

Hardage, B. A., 1985, Vertical seismic profiling: part A: principles, Pergamon Press.

Harris, J. M, and Rector, J. W., Lazaratos, S. K., and Van Schaack, M.,1992, High resolution crosswell imaging of a west texas carbonate reservoir: partl-overview. To be presented at the 62nd Ann. Mtg. of SEG, New Orleans.

Lazaratos, S. K. , Rector, J. W., Harris, J. M., Van Schaack, M., 1991, High resolution imaging using crosswell reflection data, Presented at the 61st Ann. Inter. Mtg of SEG, Expanded Abstracts,1,150-153

Lazaratos, S. K. , Rector, J. W., Harris, J. M., Van Schaack, M., 1992, High resolution crosswell imaging of a west texas carbonate reservoir: part 4-reflection imaging, To be Presented at the 62nd Ann. Inter. Mtg of SEG, New Orleans.

Lee, M. W., Balch, A. H., and Parrot, K. R., 1984, Radiation from a downhole airgun source, Geophysics, 49,1, 27-36.

Rector, J. W., Lazaratos, S. K., Harris, J. M., and Van Schaack, M., 1992, Extraction of reflections from crosswell wavefields, To be presented at the 62nd Ann. Mtg. of SEG, New Orleans.

Stewart, R., and Marchisio, G., 1991, Crosswell seismic imaging using reflections, Presented at the 61st Ann. Mtg. of SEG, Expanded Abstracts, 375-378.

Van Schaack, M., J. Harris, J. Rector, and S. Lazaratos, 1992 , High resolution imaging of a West Texas carbonate reservoir: Part 2 - wavefield analysis and tomography, to be presented at the 1992 Annual Meeting of SEG, New Orleans.

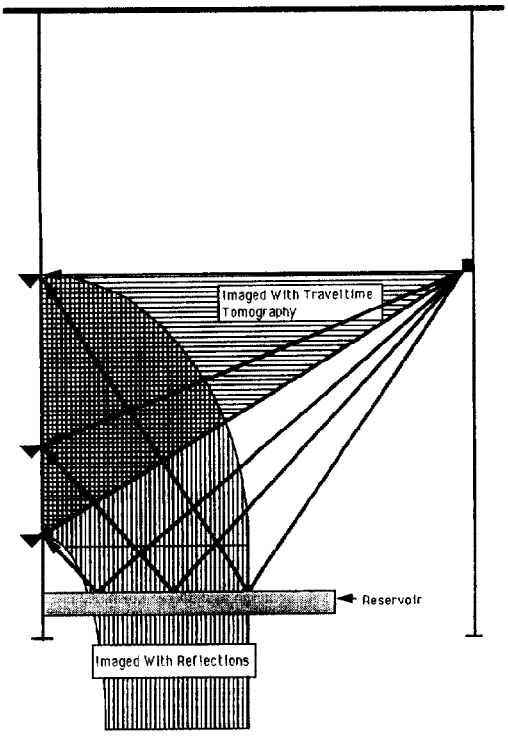

Figure 1: Subsurface region imaged with crosswell traveltime tomography compared with region imaged with crosswell reflections for a single common shot gather.

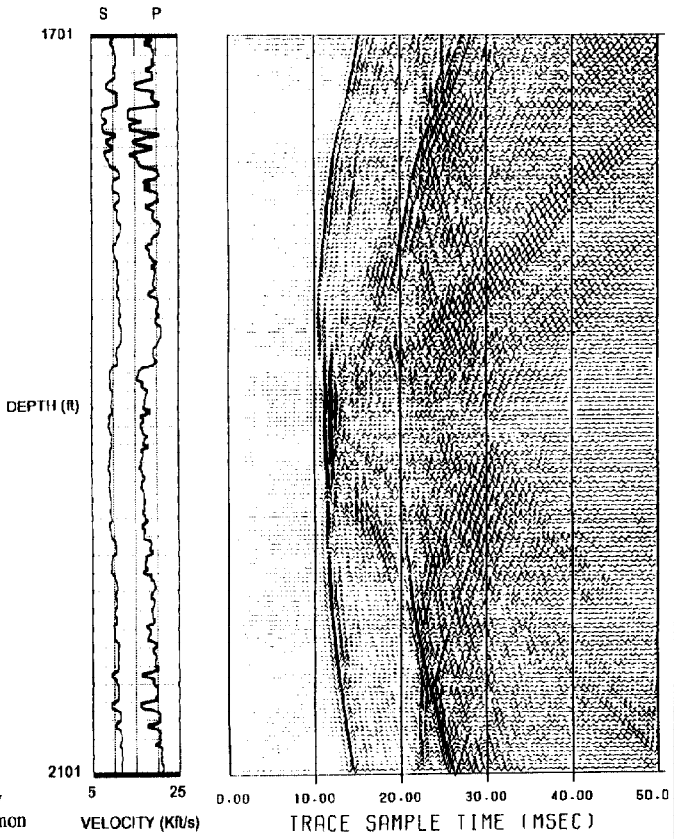

Figure 2: A typical common receiver gather from the West Texas well-to-well experiment. The receiver depth was 1904 ft, just below the top of the reservoir (the bottom of the reservoir was around 1964 ft). Source positions between 1701 ft and 2101 ft every 2.5 ft are shown.

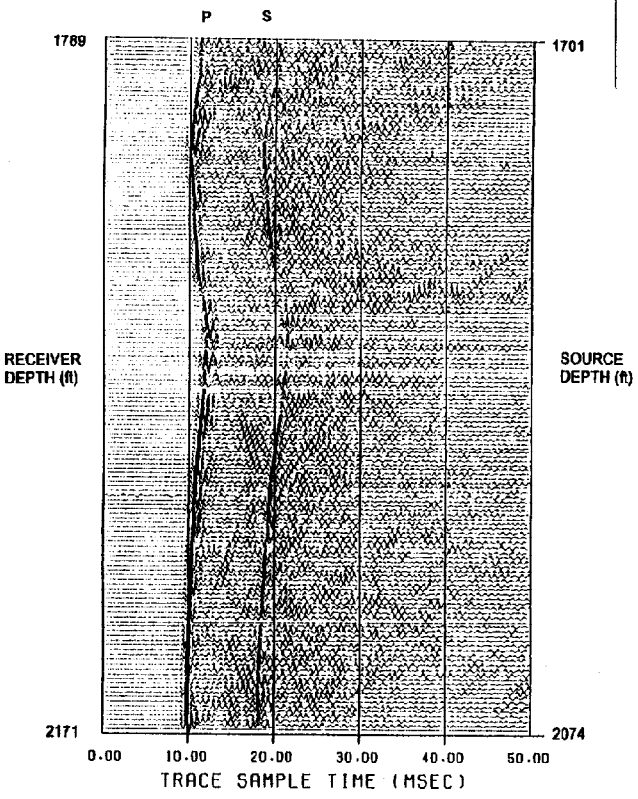

Figure 3: A common vertical offset display (source depth - receiver depth = -90 ft). Varoiations on the P and S direct arrival times correspond with velocity variations observed in the well logs.

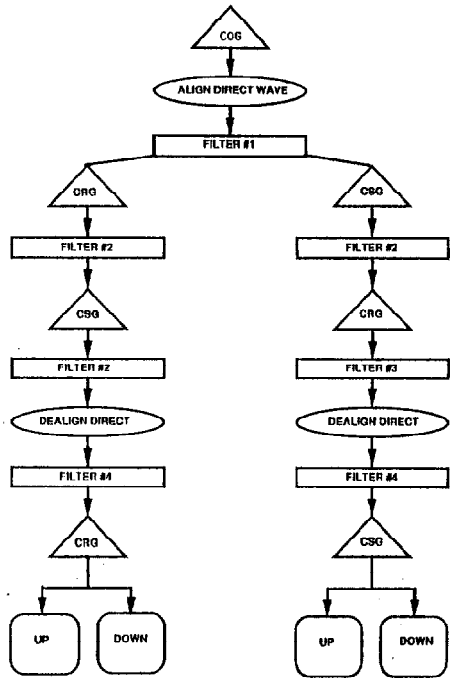

Figure 4: Wavefield separation processing flow used to extract crosswell reflections. Triangles are sorts, rectangles are multichannel filters, and ellipses are time aligning operations.

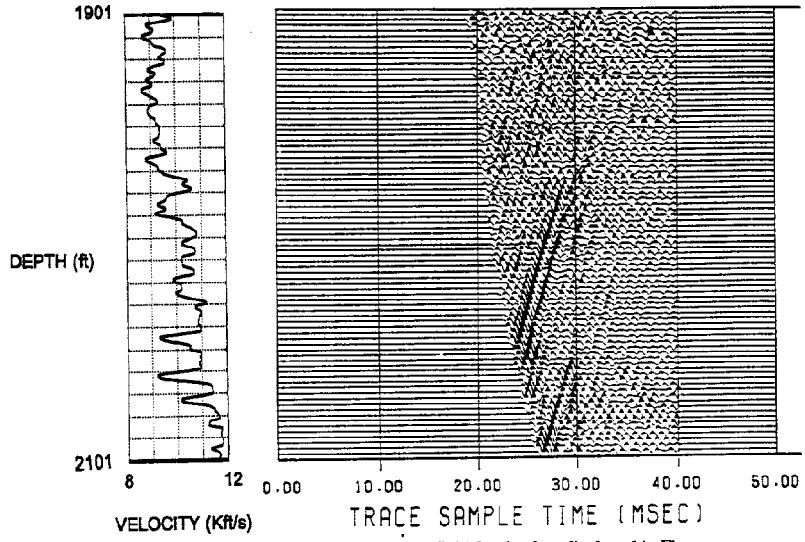

Figure 5: Upgoing S-wave reflection wavefield for the data displayed in Figure 2.